Monthly Notices of the ROYAL ASTRONOMICAL SOCIETY

Mon. Not. R. Astron. Soc. **427,** 1418–1428 (2012) doi:10.1111/j.1365-2966.2012.22062.x

Pulsational amplitude growth of the star KIC 3429637 (HD 178875) in the context of Am and ρ Pup stars

Simon J. Murphy,[1⋆] A. Grigahcène,[2,3] E. Niemczura,[4] D. W. Kurtz[1] and K. Uytterhoeven[5,6]

[1]*Jeremiah Horrocks Institute, University of Central Lancashire, Preston PR1 2HE*
[2]*Centro de Astrofísica, Faculdade de Ciências, Universidade do Porto, Rua das Estrelas, 4150-762 Porto, Portugal*
[3]*Kavli Institute for Theoretical Physics and Department of Physics Kohn Hall, University of California, Santa Barbara, CA 93106, USA*
[4]*Astronomical Institute, Wrocław University, Kopernika 11, 51-622 Wrocław, Poland*
[5]*Instituto de Astrofísica de Canarias (IAC), Calle Via Lactea s/n, 38205 La Laguna, Tenerife, Spain*
[6]*Dept. Astrofísica, Universidad de La Laguna (ULL), Tenerife, E-38206 La Laguna, Spain*

Accepted 2012 September 5. Received 2012 September 4; in original form 2012 August 1

ABSTRACT

KIC 3429637 (HD 178875) is a δ Sct star whose light curve shows continuous pulsational amplitude growth in *Kepler* mission photometry. Analysis of the three largest amplitude peaks in the Fourier transform indicates different growth rates for all three. We have ruled out instrumental causes, and determine the amplitude growth to be intrinsic to the star. We calculate time-dependent convection models and compare them with the observations. We confirm earlier characterizations that KIC 3429637 is a marginal Am star through the analysis of new spectroscopic data. With the data presently available, a plausible cause of the amplitude growth is increasing pulsational driving as evolutionary changes shift the He II driving zone deeper in this ρ Puppis star. If this model is correct, then we are watching real-time stellar evolutionary changes.

Key words: stars: chemically peculiar – stars: individual: HD 178875 – stars: oscillations – stars: variables: δ Scuti.

1 INTRODUCTION

The δ Sct stars are low-overtone pressure mode pulsators on or near the main sequence between spectral types A2V to F0V and A3III to F5III (Kurtz 2000), whose pulsation frequencies range from 3 to 80 d^{-1} (i.e. 18 min to 8 h in period). Their pulsations are driven by the opacity (κ) mechanism operating on the He II partial ionization zone. These intermediate-mass (1.5–2.5 $M_\odot$) stars are mostly Population I (Pop I) stars, but some Pop II δ Sct stars do exist and are known as SX Phe variables (see e.g. Templeton, Basu & Demarque 2002).

The δ Sct instability strip is located at the junction between the classical Cepheid instability strip and the main sequence. It is not populated solely with δ Sct variables with normal spectra, however. The δ Sct stars have as their neighbours the following: the photometrically less variable, chemically peculiar, classical metallic-line (Am) stars; the marginal Am (Am:, pronounced 'Am colon') stars with slightly milder abundance anomalies; the early or hot Am stars; the ρ Pup stars (evolved Am stars); the Ap stars (where the 'p' means peculiar); the γ Dor stars; the λ Boo stars; and the 'normal' A-stars. This paper concerns KIC 3429637, a ρ Pup star showing δ Sct pulsations.

1.1 The Am stars

The classical Am stars are those whose Ca II K-line types appear too early for their hydrogen line types, and metallic-line types appear too late, such that the spectral types inferred from the Ca II K line and metal line differ by five or more spectral subclasses. Such stars are therefore commonly given three spectral types, e.g. Am kA8hA9mF3, corresponding to the K line, hydrogen lines and metallic lines, respectively. The Am group makes up a significant fraction of late A-stars – up to 50 per cent at A8 (Smith 1973; Smalley et al. 2011), and features abundance anomalies typically of factors of ± 10 (Abt 2009). Historically, the classical Am stars were thought not to pulsate, but with the micromagnitude photometric precision of the space-based *Kepler* mission six of the 10 known Am stars in the *Kepler* field of view are observed to pulsate (Balona et al. 2011a), and Smalley et al. (2011) found 200 of 1600 metallic-line A and F dwarfs to be pulsating from SuperWASP data.

The Am stars rotate sufficiently slowly that turbulent motions do not prevent gravitational settling of helium (Baglin et al. 1973). When enough helium is drained from the He II partial ionization

⋆E-mail: smurphy6@uclan.ac.uk

zone, the star no longer pulsates. Meanwhile, ions with absorption lines near the peak wavelength of the photon energy distribution are radiatively levitated towards the surface, and others, notably He, C, Ca and Sc, gravitationally settle, thus providing the abundance anomalies (Kurtz 1989).

The marginal Am stars show fewer than five spectral subclasses between the Ca II K and metallic lines. Such stars are therefore less extreme examples of the classical Am stars, with milder abundance anomalies. Kurtz (1978) showed that the majority of the Am: stars lie at the blue edge of the δ Sct instability strip (his fig. 2), which makes them difficult to distinguish from the 'hot Am stars' whose primary characteristics are Am anomalies in stars hotter than A4. Marginal Am stars are also found at the cool edge of the instability strip, however, with spectra similar to the historical δ Del stars. We refer the reader to Gray & Garrison (1989) for a discussion of why the δ Del classification has been dropped and why the evolved Am stars are now known as ρ Pup stars.

Kurtz (1978) presented members of the ρ Pup class, which also pulsate. A particularly good case study of a ρ Pup star that is also a high-amplitude δ Sct star is that of HD 40765 (Kurtz et al. 1995). There it was found that spectral peculiarities still remain in the presence of a peak-to-peak surface radial velocity range of 14 km s^{-1}.

1.2 Models of pulsating Am stars

The introduction of time-dependent convection in the modelling of δ Sct star pulsations was a major step towards a quantitative comparison between theory and observations. Dupret et al. (2004, 2005) have successfully explained the red edge of the δ Sct instability strip by using these models. This approach was successfully applied to three δ Scuti stars by Dupret et al. (2005). The δ Sct stars observed by *Kepler* offer a higher level test for the theory. In this work we apply time-dependent convection models to a δ Sct star observed by *Kepler* for the first time.

Before we move on to the specific case of KIC 3429637, let us discuss the issue of pulsation coincident with metallicism, i.e. of the ρ Pup stars. In the Am stars it was thought that there should be insufficient helium left in the He II partial ionization zone for δ Sct pulsations to be driven, but this is becoming increasingly doubted (e.g. Catanzaro & Balona 2012). Kurtz (1989) discussed the theoretical exclusion of metallicism and pulsation in detail before announcing the first case of an extreme classical Am star showing δ Sct pulsations. It appears that pulsation in chemically peculiar stars with pulsation velocities of several hundred m s^{-1} can be so laminar that turbulence of the order of cm s^{-1} is not generated. If turbulence were generated, the diffusion process would become ineffective and the stars would become homogenized. Turcotte et al. (2000) addressed the issue, noting that it is velocity gradients that generate turbulence, and not the speed of displacement itself – fast but uniform displacement will not become turbulent. Their models, the New Montreal Models, which take diffusion of elements up to Ni into account, find stable stars with He abundances as low as 0.114 at 750 Myr. Specifically, He is still substantially present in the He II driving region in these models, and the iron-peak-element opacity bump is increased relative to standard models and contributes to excitation of longer period modes. As the stars evolve, they begin to pulsate naturally [i.e. without invoking dredge-up or hypothetical mass-loss (Turcotte et al. 2000)] because of the way that radius expansion causes the He II ionization zone to shift inward in mass fraction where more residual He is present (Cox, Hodson & King 1979). The evolution leads to an increase in period of observed pulsation modes, and Turcotte et al. concluded that generally the effect of diffusion is to stabilize against p-mode pulsations but excite g modes. No extensive observational study covering a large sample of stars has been carried out to investigate pulsation frequency ranges in light of abundance anomalies.

In spite of all the strengths of diffusion theory (see e.g. Kurtz 2000), the diffusion models still fail to reproduce the recent observations of the commonality of pulsating Am stars (Smalley et al. 2011) satisfactorily, though we note that the disparity is not as great as it seems because 24 per cent of their 'pulsating Am' sample were actually 'Fm δ Del' stars, and that pulsations are expected to occur naturally in these evolved stars according to modern diffusion models. We refer the reader to the work of Balona et al. (2011b) for further discussion and observations on the edges of the instability strip for pulsating Am stars.

1.3 The *Kepler* space mission

The *Kepler* space mission features an array of 42 CCDs covering a 115 deg^2 area of the sky between the constellations of Cygnus and Lyra. It captures white-light photometric data from ∼150 000 stars, with the objective of detecting transiting planets that orbit within the habitable zone (Koch et al. 2010). The attained precision is around the micromagnitude level, and, with a duty cycle > 92 per cent, the mission offers vast advances in astrophysics through the study of stellar pulsations. With photometry alone, transiting studies only yield the ratio of the planet and host-star radii, but asteroseismology can determine stellar radii to within ∼1 per cent in some cases (Gilliland et al. 2010). Keeping that in mind, about 1 per cent of observations are allocated to asteroseismology.

Kepler data are available in two cadences: long cadence (LC) with effective 29.4-min integrations and short cadence (SC) with 58.9-s integrations. The near-continuous observations are interrupted every 32 d (one 'month') for data downlinking, and every three months corresponds to one quarter of *Kepler*'s 372.5-d heliocentric, Earth-trailing orbit. LC data are therefore available in quarters (denoted Qn), and SC data are further subdivided into months (denoted Qn.m). Each quarter the satellite performs a roll to keep its solar panels pointed towards the Sun and its radiator pointed towards deep space. Stars subsequently fall on to a different detector module when the symmetrical focal plane rotates. The unfortunate failure of module 3 early in the mission means that a small fraction (∼4/21) of the field of view is only observable for three quarters of the year.

2 PHOTOMETRIC OBSERVATIONS

Kepler data are available in abundance for KIC 3429637, which is the ninth brightest in the δ Sct working group of the Kepler Asteroseismic Science Consortium (KASC). LC public data are available from Q1 through Q8, and SC public data are available for each month of Q7 and Q8. The LC data, with just over 30 000 data points covering 670.33 d, have a duty cycle of 91.4 per cent. The light curve for the Pre-search Data Conditioned (PDC) LC data is displayed in Fig. 1, from which it is immediately clear that the amplitude of the light variation is growing with time. We used only the least-squares version of the PDC pipeline (i.e. PDC-LS).

There are two obvious potential sources of the apparent amplitude growth: (1) the amplitude growth is intrinsic to the star, i.e. astrophysical; and (2) the amplitude growth is in some way instrumental. PDC data are not created to facilitate asteroseismology, but rather to prepare the data for planet searches. As such, the data are not to be used for asteroseismology without caution that the pipeline

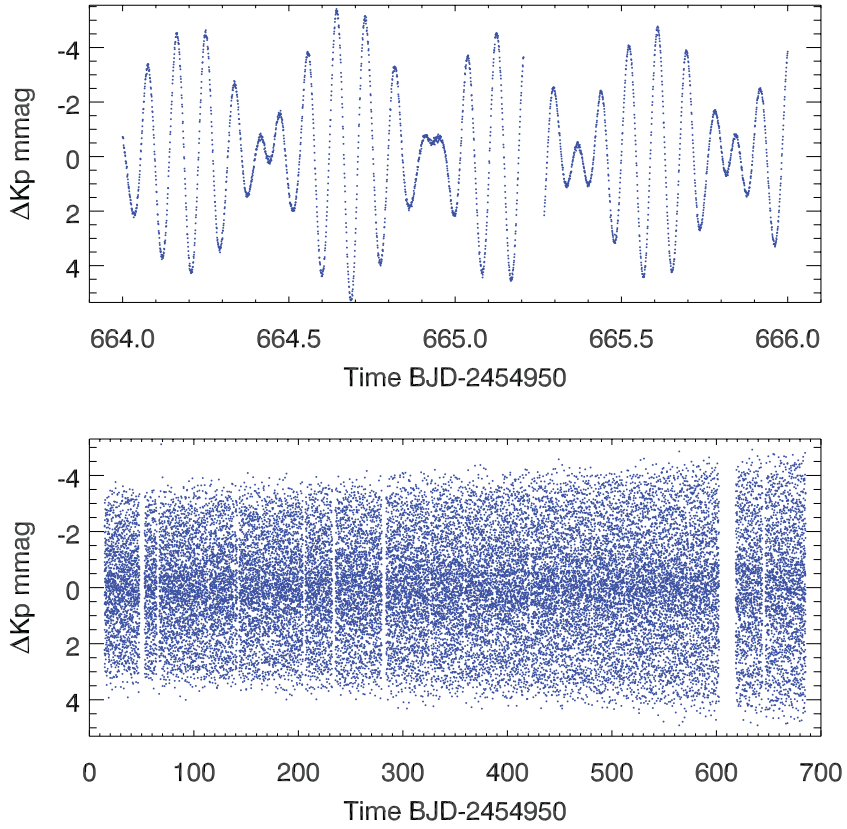

Figure 1. Upper panel: the δ Sct pulsations of KIC 3429637 in SC PDC from Q8. Kp denotes *Kepler* magnitude, and BJD is Barycentric Julian Date. Lower panel: the unedited light curve of the LC PDC data from Q1 to Q8. The amplitude of light variation is clearly growing with time, as can be seen from the unresolved envelope of the pulsations.

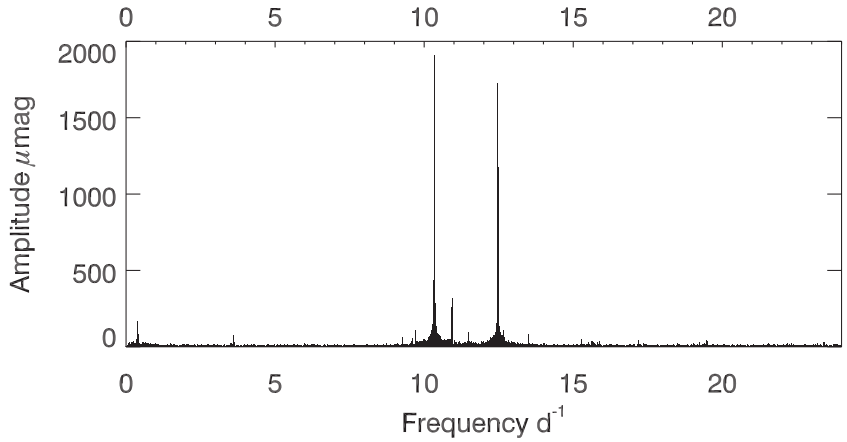

Figure 2. The Fourier transform of the unedited Q5 LC time string. The three highest amplitude peaks, in descending amplitude order, are f_1, f_2 and f_3.

might modify stellar variability. To test whether the pipeline caused the amplitude growth we compared the PDC data to the simple aperture photometry (SAP) data, for which only basic calibration has been performed and which is deemed suitable for asteroseismology, provided that instrumental trends are corrected for. Since instrumental trends generally affect low frequencies only, these are not an issue in the periodogram at the frequencies of pulsation shown in the Fourier transform of the data in Fig. 2. The amplitudes of the pulsations in the PDC data were compared to the uncorrected SAP data, by means of a non-linear least-squares fit of the frequencies to each quarter of data using the software package PERIOD04 (Lenz & Breger 2004). The amplitude growth was the same in both data sets.

The star has two dominant frequencies ($f_1 = 10.337\,\mathrm{d}^{-1}$ and $f_2 = 12.472\,\mathrm{d}^{-1}$), with amplitudes growing between 1.5 and 2.5 mmag, and a third mode that lies between them ($f_3 = 10.936\,\mathrm{d}^{-1}$) with an amplitude of $\sim$0.3 mmag – observable without any pre-whitening. These frequencies are typical for δ Sct stars. As an additional check that the amplitude growth is astrophysical and not instrumental, the amplitude of that third peak was tracked across multiple quarters for comparison. It was found that although the two main peaks continued to grow in amplitude across all quarters, f_3 showed a

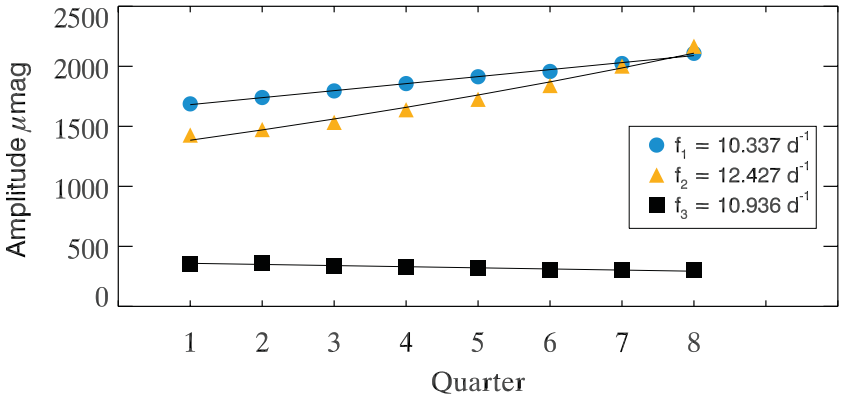

Figure 3. The growth of amplitude of f_1 and f_2, and decrease in amplitude of f_3 in LC PDC-LS flux as a function of time. Linear fits are shown for f_1 and f_3, and an exponential fit is shown for f_2. Errors on amplitude are of the order of a few micromagnitudes, and are much smaller than the plot symbols.

continual decrease in amplitude, as seen in Fig. 3. *This proves that the growth in amplitude of the light variation is astrophysical*. In addition to these three main frequencies, some ∼40 statistically significant peaks with lower amplitudes exist in the data. We tracked the amplitudes of only the next four highest amplitude modes, and have hence tracked all modes for which modelling was performed (see Section 6). The amplitudes of these four modes, not shown in Fig. 3, show changes of no more than 30 μmag across the eight quarters and the changes appear to be noise dominated, so the amplitudes of peaks with lower statistical significance were not tracked.

The optimum aperture for a star is defined such that the signal-to-noise ratio of the light captured from that star is maximized. This does not, therefore, capture all light from that star, because pixels further from the centre of the star contain less of the star's light and therefore relatively higher noise levels. It is possible, as a direct consequence of the choice of optimum aperture, that slightly more light from this star is being captured in each quarter and slightly less of a neighbouring star that is contributing towards the total light, which would create the effect of amplitude growth of *all* pulsation frequencies in the star's Fourier spectrum. Although not all modes grow in amplitude, a check is necessary. The Kepler Input Catalogue (KIC; Latham et al. 2005; Brown et al. 2011) lists the contamination for this star to be 0.037, meaning that about 3.7 per cent of the light in the aperture of this star comes from one or more neighbours rather than the target star itself. To rule out the hypothesis that the amplitude growth is due to changing flux fractions of any neighbour, we took the target pixel light curves of Q1 to Q5 and defined a mask for each one that covered every pixel available for the star for that quarter. We found that just as for the PDC LS pipeline data, with our custom mask the amplitudes of the dominant modes grew each quarter and the amplitude of the third mode that lies between them continued to decrease.

In the Catalogue of the Components of Double and Multiple Stars (CCDM; Dommanget & Nys 1994), KIC 3429637 is listed as a double star with a separation of 1.58 arcsec. The primary has $V = 7.8$ and the secondary has $V = 12.7$, thus the secondary has a spectral type around early K. Having a *Hipparcos* parallax of 3.75 ± 0.58 mas, the stars are well separated with an orbital period >1000 yr, so tidal effects on the primary's rotation period are unimportant. Without radial velocities, we must treat KIC 3429637 as if it were a single star. Furthermore, there is no evidence at present to rule out chance alignment.

We wish to examine the possibility that the amplitude change is caused by the secondary. According to the CCDM, the dimmer star contributes just 1 per cent of the light coming from the pair. For this dimmer star to cause an amplitude change of ∼30 per cent is impossible: one would have to remove it 30 times to exact such a change.

3 SPECTROSCOPIC OBSERVATIONS

Various methods exist for inspection of a star for chemical peculiarity, and definitions of peculiarity in the literature are complex. In his Am star review, Conti (1970) summarized the peculiarities as 'deficient Ca (Sc) or overabundant heavier elements, or both'. Indeed, Conti (1965) used the line depth ratio of Sc II λ4246.8/Sr II λ4215.5 as an indicator of peculiarity and Smith (1970) went further and used another criterion Sc II λ4320.7/Y II λ4309.6 because of the potential for blending of the Sc II line with the Fe I line (at λ4247.3) in fast rotators; Smith (1970) noted that a substantial fraction of Am stars may be nearly normal in Sc and Ca. Modern abundance surveys are consistent with long-established characterizations: Gebran et al. (2010) found that 'All Am stars in the Hyades are deficient in C and O and overabundant in elements heavier than Fe but not all are deficient in calcium and/or scandium.'

Another method for detection of peculiarity is the Strömgren Δm_1 index. A-stars with negative Δm_1 indices are commonly Am stars, with more negative values indicating a more chemically peculiar star. Using *uvby* parameters for KIC 3429637 from Olsen (1983) and Hauck & Mermilliod (1998) ($b - y = 0.189$, $m_1 = 0.215$, $c_1 = 0.849$), noting that both sources agree to that precision, the Δm_1 index for this star was calculated using table 1 of Crawford (1979) for calibration as $\Delta m_1 = -0.028$, which indicates an Am/Am: star. Our evaluation is consistent with that of Abt (1984), who classified the star as Am(F2/A9/F3) – a marginal Am star given that the metallic-line type and Ca II K line type differ by fewer than five spectral subclasses. We note that although the Crawford Δm_1 calibration is for main-sequence stars, it may also be applied to evolved stars.

Atmospheric parameters for KIC 3429637 were calculated by Catanzaro et al. (2011) as part of their spectroscopic survey of potential *Kepler* asteroseismic targets in the δ Sct and γ Dor instability strips. They estimated an equivalent spectral type of F0 III (from fundamental parameters), $v \sin i = 50 \pm 5$ km s^{-1}, and used a variety of methods to determine $T_{\rm eff}$ and $\log g$. The weighted mean of their values for $T_{\rm eff}$ and $\log g$ are 7300 ± 200 K and 3.16 ± 0.25 (CGS), respectively. Catanzaro et al. also computed masses for this star: a canonical value of $3.6^{+0.7}_{-0.6}\,{\rm M}_\odot$ and a non-canonical value (that is, with convective overshooting: $\lambda_{\rm OV} = 0.2\,H_p$) of $3.2^{+0.6}_{-0.5}\,{\rm M}_\odot$. They

Table 1. The elemental abundances for KIC 3429637 as compared to the solar values of Asplund et al. (2009). Columns 4 and 5 display the abundances of this star and the Sun, respectively, with their standard deviations. For those elements in column 4 whose abundances were determined from only one or two lines, an accurate uncertainty estimate cannot be made so we provide the mean uncertainty of our other abundances (0.12) instead. Column 6 is the difference between columns 4 and 5. Column 7 contains [M/H] for the normal A-stars from Gebran et al. (2010) for the elements they analysed. In their paper, these abundances were relative to the solar values of Grevesse & Sauval (1998), but here we correct them to the latest and most precise abundances: Asplund et al. (2009). Column 8 contains the difference between the abundances of this star and a normal A-star. The final column is like column 8, but with a metallicity correction applied – it represents the difference between KIC 3429637 and a normal star of the same Fe/H (see in-text explanation, Section 3.3).

Element	Z	No. of lines	Abundance	Solar value	[M/H]	A-stars	ΔM	$\Delta M_{\rm corr}$
C	6	6	8.03 ± 0.16	8.43 ± 0.05	-0.40 ± 0.17	-0.06	-0.25	-0.49
Na	11	1	6.07 ± 0.12	6.24 ± 0.04	-0.17 ± 0.13	0.29	-0.37	-0.04
Mg	12	6	7.53 ± 0.15	7.60 ± 0.04	-0.07 ± 0.16	0.13	-0.22	0.07
Si	14	4	7.32 ± 0.17	7.51 ± 0.03	-0.19 ± 0.17	0.39	-0.54	-0.08
S	16	1	7.67 ± 0.12	7.12 ± 0.03	0.55 ± 0.12	–	–	–
Ca	20	11	6.34 ± 0.09	6.34 ± 0.04	0.00 ± 0.10	0.04	-0.02	-0.03
Sc	21	11	2.97 ± 0.10	3.15 ± 0.04	-0.18 ± 0.11	-0.25	0.09	-0.38
Ti	22	29	4.82 ± 0.13	4.95 ± 0.05	-0.13 ± 0.14	0.15	-0.21	-0.11
V	23	2	4.43 ± 0.12	3.93 ± 0.08	0.50 ± 0.14	–	–	–
Cr	24	25	5.50 ± 0.20	5.64 ± 0.04	-0.14 ± 0.20	0.17	-0.28	-0.05
Mn	25	6	5.24 ± 0.14	5.43 ± 0.05	-0.19 ± 0.15	0.13	-0.36	-0.16
Fe	26	80	7.35 ± 0.11	7.50 ± 0.04	-0.15 ± 0.12	0.19	-0.34	0.00
Ni	28	17	6.43 ± 0.12	6.22 ± 0.04	0.21 ± 0.13	0.36	-0.12	0.39
Cu	29	2	3.92 ± 0.12	4.19 ± 0.04	-0.27 ± 0.13	–	–	–
Zn	30	2	4.37 ± 0.12	4.56 ± 0.05	-0.19 ± 0.13	–	–	–
Sr	38	2	3.97 ± 0.12	2.87 ± 0.07	1.10 ± 0.14	0.39	0.81	1.41
Y	39	3	2.94 ± 0.01	2.21 ± 0.05	0.73 ± 0.05	0.57	0.19	1.01
Zr	40	3	2.98 ± 0.03	2.58 ± 0.04	0.40 ± 0.05	0.62	-0.20	0.10
Ba	56	3	3.08 ± 0.13	2.18 ± 0.09	0.90 ± 0.16	–	–	–
La	57	1	0.92 ± 0.12	1.10 ± 0.04	-0.18 ± 0.13	–	–	–

estimated the luminosity to be $20 \pm 6\,L_{\odot}$. Additional parameters from the KIC, roughly derived from broad-band photometry, are $R = 4.1\,R_{\odot}$ and [Fe/H] = 0.12. It is immediately apparent from the luminosity class and $\log g$ parameters that the star is a giant, and thus an evolved Am, or ρ Pup, star. A comparison of the m_1 value of this star with those studied by Kurtz (1976, his fig. 3) strongly implies that this star is of the ρ Pup type. We return to this in Section 4.

3.1 New spectroscopic observations

A medium-resolution optical spectrum of the investigated object was obtained using the cross-dispersed, Fibre-fed Échelle Spectrograph (FIES) on the 2.5-m Nordic Optical Telescope, at Roque de los Muchachos, La Palma during the run of 2010 August 3–5 (proposal: 61-NOT7/10A). FIES offers an optical spectrum from 3700 to 7300 Å, with a spectral resolution of 46 000 in a single exposure. The signal-to-noise ratio of the spectrum is about 100 at 5500 Å.

The spectrum was reduced using standard procedures of FIEStool, which consists of bias subtraction, extraction of scattered light produced by the optical system, division by a normalized flat-field and wavelength calibration. After reduction, the spectrum was normalized to the continuum by using SPLAT, the spectral analysis tool from the Starlink project (Draper et al. 2005).

3.2 Atmospheric parameters' determination

To perform an abundance analysis, one needs to determine an appropriate atmospheric model of the star, which requires the knowledge of its effective temperature $T_{\rm eff}$, surface gravity $\log g$ and metallicity. The necessary atmospheric models were computed with the line-blanketed local thermodynamic equilibrium (LTE) ATLAS9 code (Kurucz 1993a), which treats line opacity with opacity distribution functions. The synthetic spectra were computed with the SYNTHE code (Kurucz 1993b) over the wavelength ranges 4000–5850 and 6100–6800 Å, excluding those segments contaminated with telluric lines. Both codes, ATLAS9 and SYNTHE, were ported under GNU Linux by Sbordone (2005) and are available online.[1] The stellar line identification and the abundance analysis were performed on the basis of the line list from Castelli & Hubrig (2004).[2]

We derived $T_{\rm eff}$ for KIC 3429637 using the sensitivity of hydrogen line wings to temperature, following the method proposed by van't Veer-Menneret & Megessier (1996). The effective temperature was estimated by computing the ATLAS9 model atmosphere which gives the best match between the observed Hδ, Hγ, Hβ and Hα line profiles and those computed with SYNTHE. The same value of $T_{\rm eff}$ was obtained from the analysis of iron lines. In this method effective temperature, surface gravity and microturbulence (ξ) are determined by the comparison of the abundances obtained from neutral and ionized iron lines. The analysis is based on Fe lines because they are the most numerous in the stellar spectrum. In general, we require that the abundances measured from Fe I and Fe II lines yield the same result. The absorption lines of Fe I depend mainly on $T_{\rm eff}$, ξ and metallicity, and are practically independent of $\log g$, whereas the Fe II lines are mostly sensitive to $\log g$. First, we adjust ξ until we see no correlation between iron abundances and line intensity for the Fe I lines. Secondly, $T_{\rm eff}$ is changed until we see

[1] wwwuser.oat.ts.astro.it/atmos/

[2] http://wwwuser.oat.ts.astro.it/castelli/grids.html

Table 2. Fundamental atmospheric parameters determined from the FIES spectrum.

$T_{\rm eff}$ (K)	$\log g$ (CGS)	ξ (km s^{-1})	$v \sin i$ (km s^{-1})
7300 ± 100	3.0 ± 0.1	4.0 ± 0.5	51 ± 1

no trend in the abundance versus excitation potential of the atomic level causing the Fe I lines. ξ and $T_{\rm eff}$ are not independent of each other. Then $\log g$ is obtained by fitting the Fe II and Fe I lines and by requiring the same abundances from both neutral and ionized lines.

The abundances of chemical elements were determined by the spectrum synthesis method. Our analysis follows the methodology presented in Niemczura, Morel & Aerts (2009) and relies on an efficient spectral synthesis based on a least-squares optimization algorithm. This method allows for the simultaneous determination of various parameters involved with stellar spectra and consists of the minimization of the deviation between the theoretical flux distribution and the observed normalized one. The synthetic spectrum depends on the stellar parameters, such as $T_{\rm eff}$, $\log g$, ξ, $v \sin i$ and the relative abundances of the elements. Some of these parameters have similar influence on stellar spectra and have to be known before the determination of the abundances of chemical elements. $T_{\rm eff}$, $\log g$ and ξ are the input parameters. All other aforementioned parameters can be determined simultaneously because they produce detectable and different spectral signatures. The $v \sin i$ values are determined by comparing the shapes of observed metal line profiles with the computed profiles, as shown by Gray (2005).

For chemical abundance analysis we used short segments of the spectrum to isolate individual spectral features, and in a few cases, some blended features. In the case of blended lines, more than one chemical element can influence the line profile. Only the most important elements for characterizing Am star peculiarities were considered. Every selected part of the spectrum was analysed by the spectrum synthesis method described above. We iteratively adjusted radial velocity, $v \sin i$, and chemical abundances until the determined parameters remained the same within 2 per cent for three consecutive iterations, thus determining the closest match between the calculated and observed spectrum. Finally, we determined the average values of radial velocity, $v \sin i$, and abundances of 20 elements with error estimates (Table 1). Table 2 summarizes our determined atmospheric parameters, and we plot our spectrum against comparisons in Fig. 4.

3.3 Discussion of spectroscopic results

The line ratios of Conti (1965) and Smith (1970) were inconclusive on the Am: nature of the star, necessitating the full abundance analysis (Table 1). We note normal Ca and nearly normal Fe, but slightly deficient Sc, strongly deficient C, and highly overabundant Sr, Y and Ba, which would collectively confirm that the star is chemically peculiar. However, observations of Gebran et al. (2010) suggest that even normal A-stars are overabundant in Sr, Y and Zr with respect to solar values. This effect of overabundant heavy elements can have multiple origins as discussed in the following.

(1) The study of Gebran et al. focused on the Hyades cluster, and those cluster stars could be systematically enriched in heavier elements. The abundances of nearly all heavier elements are known to be correlated with iron (Hill & Landstreet 1993). The [Fe/H] of the Hyades cluster is not well agreed upon. Boesgaard & Friel (1990) determined a supersolar metallicity $\langle[{\rm Fe/H}]\rangle = 0.127 \pm 0.022$ dex; however, Varenne & Monier (1999) found a much lower value of -0.05 ± 0.03 dex when investigating 29 F dwarfs. Gebran et al. themselves find ${\rm Fe/H} = 0.19$ dex above solar. A recent independent calculation (Carrera & Pancino 2011) based on three K giants yields $\langle[{\rm Fe/H}]\rangle = +0.11 \pm 0.01$ dex and is close to the mean of previous studies collated by those authors. We may therefore safely conclude at least a slightly supersolar Fe abundance and that correlation with Fe is a contributor.

(2) Using the Sun as a standard star has the weakness of assuming that the Sun is typical. Meléndez et al. (2009) found the Sun to be depleted in refractory elements by ∼20 per cent relative to volatile elements compared to solar twins. Specifically, the lighter, volatile elements (e.g. C, N and O) are enriched by ∼0.05 dex and the heavier, refractory elements depleted by ∼0.03 dex. Their findings were confirmed in another study (Ramírez, Meléndez & Asplund 2009), and the hypothesis that planetary formation is the cause is independently theoretically supported (Chambers 2010). The peculiar solar abundance therefore also contributes to the

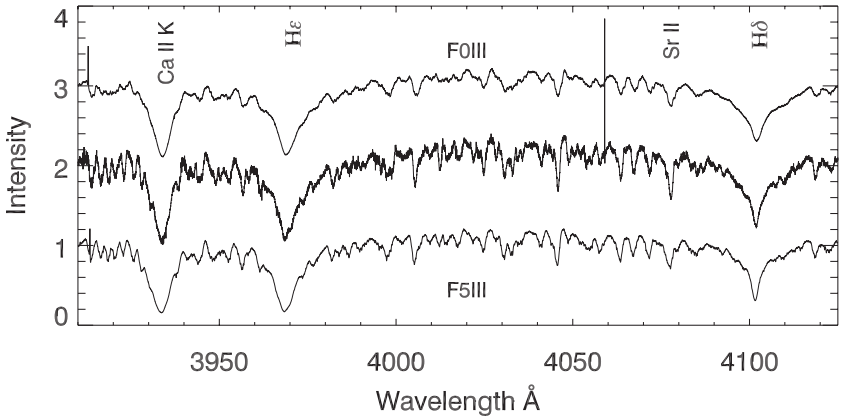

Figure 4. Spectrum of KIC 3429637 (centre) with two comparisons: the F0 III star HD 7312, and the F5 III star HD 65925, though neither is an MK-standard star. Catanzaro et al. (2011) listed KIC 3429637 as F0 III m. The hydrogen line type is a good match to ∼F0/A9. Despite being of the Am type, note that the Ca II K line is no weaker than the F0 comparison (cf. Table 1, in which calcium is completely normal). The metal lines are much stronger, though, and are even stronger than the F5 comparison. In particular, the Sr II λ4077 line is much deeper, owing to the Am nature. The comparison spectra were obtained at 'http://www.eso.org/sci/observing/tools/uvespop/field_stars_uptonow.html', normalized at 3910.0 Å and vertically separated by 1 unit.

apparent overabundance of heavy elements in normal A-stars, and we may assume that a specific physical effect in A-star photospheres is not at play.

(3) One must also consider that the abundances of heavier elements are derived from fewer lines, and are therefore at greater risk of having erroneous values caused by blends.

Nevertheless, for those elements that were studied by Gebran et al. we also show the difference between KIC 3429637 and normal A-star abundances, relative to the Sun in Table 1. Mn, Ni, Sr and Ba are strongly correlated with Fe (Gebran, Monier & Richard 2008), and Y and Zr increase rapidly with Fe/H (Gebran et al. 2010), thus the chemical peculiarities of KIC 3429637 would be even more pronounced were it not for its low iron abundance. Therefore in the final column of Table 1 we tentatively provide the abundance differences as if KIC 3429637 had the same Fe/H as the mean value of the 'normal' A-stars to which we are comparing, namely [Fe/H] = 0.19. The correction is calculated from the data tables provided in the online material of Gebran et al. (2010). Since A-stars are known to show large star-to-star variations in abundances compared to F-stars (Gebran, Monier & Richard 2008), the correlation between [M/H] and [Fe/H] is not always tight, hence the 'tentative' provision. Importantly, the elements for which the correlation is tighter are those that are the most peculiar. Fossati et al. (2008b) found that there is no temperature effect on abundance patterns, thus we need not worry about any temperature difference between KIC 3429637 and the mean of the A-stars against which we are comparing.

We did not take non-LTE effects into account in our calculations, yet these effects can be important. Given the importance of calcium in Am star spectra, we considered non-LTE corrections for this element, but they are small (Mashonkina, Korn & Przybilla 2007). For iron, non-LTE corrections are significant (0.2–0.3 dex) for Fe I, but not Fe II, and are positive (Rentzsch-Holm 1996). The corrections would bring our Fe abundance closer to the solar value. Conversely, corrections for carbon are negative (Rentzsch-Holm 1996) and would further exaggerate the carbon deficiency seen in this star and expected in Am stars.

All three of our $T_{\rm eff}$, $\log g$ and $v \sin i$ determinations agree extremely well with the weighted means of those presented in Catanzaro et al. (2011), and ξ is slightly high for a star of this temperature (Takeda et al. 2008). We note, however, that in Am stars ξ is expected to be slightly higher than in normal stars (Coupry & Burkhart 1992; Gebran & Monier 2007). The former authors pointed out that the ξ distribution reaches a maximum around A5, where the angular rotational velocity distribution also reaches a maximum. This could implicate rotational instabilities in generating microturbulence, but if that were true Am stars would not be observed to have higher ξ values. Pace et al. (2006) defined the relation $\xi = -4.7\log(T_{\rm eff}) + 20.9\,{\rm km\,s^{-1}}$ for horizontal branch stars, in which radiative levitation is also important – this would give an expected ξ of $2.7\,{\rm km\,s^{-1}}$, but the relation is not appropriate for the whole main sequence, and might even be used as a diagnostic to distinguish horizontal branch stars from main-sequence stars.

The low $\log g$ value indicates that this star is evolved. Interestingly, the value of $v \sin i$ is high for an evolved Am (i.e. ρ Pup) star – Am main-sequence stars are already slow rotators, with the Am/Ap star unimodal rotation velocity distribution peaking at $\sim 60\,{\rm km\,s^{-1}}$ *after* statistical correction for inclination (Abt & Morrell 1995). During evolution, stars transfer angular momentum inward through radius expansion, slowing the surface rotation further. Hence by accepting the fact that the star is evolved, the high $v \sin i$ argues against the type of close binary system common among Am stars.[3] Instead, the hypothesis of a single A-star with a subaverage rotation velocity is favoured for this case, in which this star was rotating slowly enough to develop some peculiarities.

It is well established that a large fraction of Am stars are found in binaries and that tidal braking slows the stellar rotation, allowing diffusion to occur. With the exclusion of Sc (Fossati et al. 2008a), peculiarities are more extreme in more slowly rotating stars (Takeda et al. 2008). The observed moderate $v \sin i$ value is indeed compatible with the fact that KIC 3429637 is not an extreme Am star, as the moderate abundance anomalies imply. Notwithstanding, ρ Pup stars do not have extreme abundances, regardless of $v \sin i$. However, Stateva, Iliev & Budaj (2012) found that peculiarity is also slightly correlated with orbital eccentricity: more eccentric orbits produce more anomalous abundances, but we do not expect this to have any significance for wide binaries. Attempts to use the frequency-modulation technique of Shibahashi & Kurtz (2012) to infer orbital parameters were unsuccessful – orbital sidelobes were not present. This indicates that either the star is in a binary system with an orbital period longer than the data set, i.e. $P_{\rm orb} > 700\,{\rm d}$, or the star is not binary at all.

4 ASTROPHYSICAL CAUSE OF AMPLITUDE GROWTH

The different amplitude growth rates of each mode, visible in Fig. 3, can be used to determine a time at which the mode amplitudes were too low to be detectable from the ground, assuming that the growth rates are well behaved. A linear growth rate gave the best fit to f_1, but an exponential growth rate was more appropriate to f_2, which is growing much more rapidly than the lower frequency mode. Taking the limit of ground-based detection as 1 mmag in the amplitude spectrum, f_1 would only have become detectable $\sim$2.6 yr ago, and f_2 around 11 yr ago. We might conclude that these modes would have been undetectable in 1984 at the time when Abt spectroscopically observed the star to be metallic lined, although no photometric investigation into variability was carried out. However, Breger (2000) observed the evolved δ Sct star 4 CVn over three decades and found mode amplitudes to be unpredictable and highly variable. One high-amplitude mode in that star disappeared altogether and re-emerged with a random phase. With so few studies of amplitude growth rates, and the unpredictable behaviour seen in 4 Cvn, we cannot predict how KIC3429637 will behave or how it behaved in the past. This star is most certainly worthy of continued observation to monitor the amplitude changes.

In any case, the current rates of growth indicate that the star has (a) not been pulsating for very long, and has just crossed some instability threshold; (b) undergone large amplitude variations over long periods of time, possibly in some cyclic nature; or (c) none of the above. We do not have enough data to pursue hypothesis (b), in that we have not observed a full cycle of variation in the light curve, but since the amplitude growth is not the same for each mode, nor does it appear to be sinusoidal, the cyclical amplitude variation hypothesis is unsupported by the present evidence. If we assume this star to be like 4 CVn, then continued observations are

[3] Tidal braking is most significant when the orbital period decreases below 10 d – the tidal braking mechanism proposed by Zahn (1975) denotes that braking time-scales depend on the stellar separation to the power 8.5. This is confirmed observationally by the fact that SB2 systems are circular for periods below $\sim$8 d (Debernardi 2000).

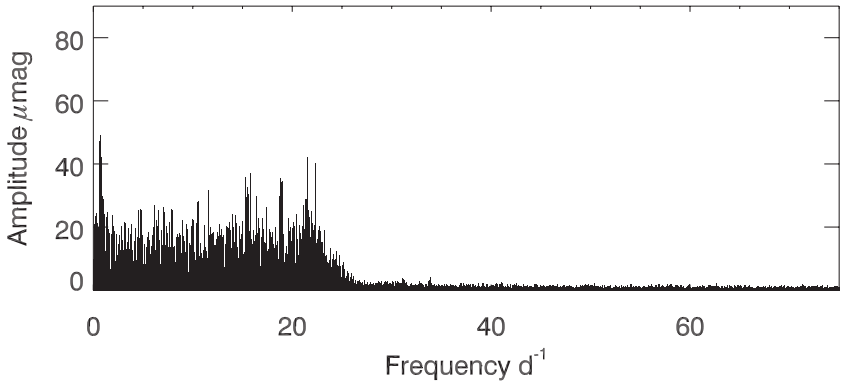

Figure 5. There is a rapid decrease in noise level at around $24\,\mathrm{d}^{-1}$. Excess noise is injected by the PDC-LS pipeline at frequencies below this limit. There are no peaks remaining below that frequency with signal-to-noise ratio >4.0, and no peaks have been removed at all above $24\,\mathrm{d}^{-1}$, hence the effect has not been caused by preferential pre-whitening. Note that here we have pre-whitened many more frequencies than were modelled in order to demonstrate the effect more clearly.

required to analyse the changing amplitudes. In the meantime, let us examine hypothesis (a) from a theoretical point of view.

Even if the pulsations are not especially laminar, the destruction of the chemical abundance anomalies may take time, such as in the case of *o* Leo A, which is an evolved Am star whose abundance anomalies have not yet been erased (Michaud, Richer & Richard 2005). KIC 3429637 could well have been a classical Am star on the main sequence, which is now at or approaching a stage of rapid evolution in which its chemical peculiarities are being erased and its pulsation amplitudes are growing. Temporal evolution of abundance anomalies is another understudied area of Am star research; KIC 3429637 would make a perfect case study. Existing studies (e.g. Abt 1979; Gebran et al. 2010) have mostly focused on multiple coeval stars in one cluster and contrasting clusters of different ages. In these cases the scatter in abundances of given elements is large enough that no real difference of any element with age is prominent. Focusing on single, regularly observed targets such as KIC 3429637 is thus potentially astrophysically rewarding.

5 NOISE IN THE RESIDUALS

Spectroscopic data show KIC 3429637 to be cool for a δ Sct pulsator, and progressively cooler A-type stars have increasingly deep surface convection zones (see Kallinger & Matthews 2010 for a discussion). We used the Q7.1 SC data to look for such a signature of granulation in the form of a rapid change in noise with frequency. We present the results in Fig. 5. After extensive investigation, the rapid decrease in noise seen between 20 and $30\,\mathrm{d}^{-1}$ was determined not to arise from granulation, but rather the noise is injected by the *Kepler* PDC-LS[4] pipeline for this particular *Kepler* quarter. It seems that approximately 15 per cent of stars in the δ Sct instability strip are afflicted with the same problem, which affects both LC and SC data, but not necessarily all quarters for a given star. A more detailed description will be given in a future publication (Murphy, in preparation).

The Q8 data for this star contain no evidence for 'granulation signature', implicating noise injection by the pipeline over an astrophysical origin. The drop in noise at $\sim 24\,\mathrm{d}^{-1}$ in SC data is characteristic for this noise injection. The Nyquist frequency of LC data prevents the drop being seen in that cadence, but the noise is still present. The new PDC maximum a posteriori (PDC-MAP) data will fix this for the LC data when the old data are reprocessed, but for now there is no implementation of MAP for SC.

[4] 'LS' describes the least-squares algorithm used by the pipeline. We refer the reader to the papers of Stumpe et al. (2012), Smith et al. (2012) and the Kepler Data Characteristics Handbook for more information on the pipeline, and to Murphy (2012) for its effect on asteroseismic analyses.

6 STRUCTURE AND OSCILLATION MODELS

In our theoretical computations we used the Code Liégeois d'Évolution stellaire CLÉS (Scuflaire et al. 2008), where the input physics is as follows: the equation of state is the superior 'CEFF' (see e.g. Christensen-Dalsgaard & Daeppen 1992); the opacity tables are OPAL opacities from Iglesias & Rogers (1996) and Alexander & Ferguson (1994) for high and low temperatures, respectively. The relative mixture of chemical composition from Grevesse & Noels (1993) was used, while the convection was treated using mixing-length theory (MLT; Böhm-Vitense 1958). Our models include neither rotation nor diffusion. For our non-adiabatic, non-radial oscillation calculations we used the MAD code (Dupret 2001), where Gabriel's treatment of time-dependent convection (TDC) has been implemented (Gabriel 1996).

We consequently produced a grid, where $\ell = 0$–3 eigenfrequency spectra are computed for each of the models. For the selection of the best model we used the maximum likelihood method as described by Grigahcène et al. (2012).

6.1 Results and discussion

Using *Kepler* data, Uytterhoeven et al. (2011) showed how A–F pulsators can have such complex frequency spectra that they are challenging targets for any asteroseismic study. We consequently need as many constraints as possible for any theoretical modelling. Although the number of detected frequencies is reduced in KIC 3429637 compared to what is usually detected in this type of star, its modelling is no less complicated.

We performed careful and detailed modelling, varying all the parameters (mass, metallicity, mixing-length parameter α_{MLT}, etc.) to obtain the combination giving the maximum value of the likelihood function. We explored different possibilities, taking into account the detected frequencies and their associated amplitudes, and the position of the star in the Hertzsprung–Russell (HR) diagram. The main requirements on our models were as follows: (1) fitting the maximum number of the observed frequencies, (2) modes should

Table 3. Properties of the best model.

M ($M_\odot$)	$T_{\rm eff}$ (K)	$\log(L/L_\odot)$	$\log g$	R ($R_\odot$)	Age (yr)	X	Z	$\alpha_{\rm MLT}$	$\alpha_{\rm Ov}$
2.178	7452	1.570	3.648	3.666	8.982E+08	0.7360	0.0149	2.0	0.2

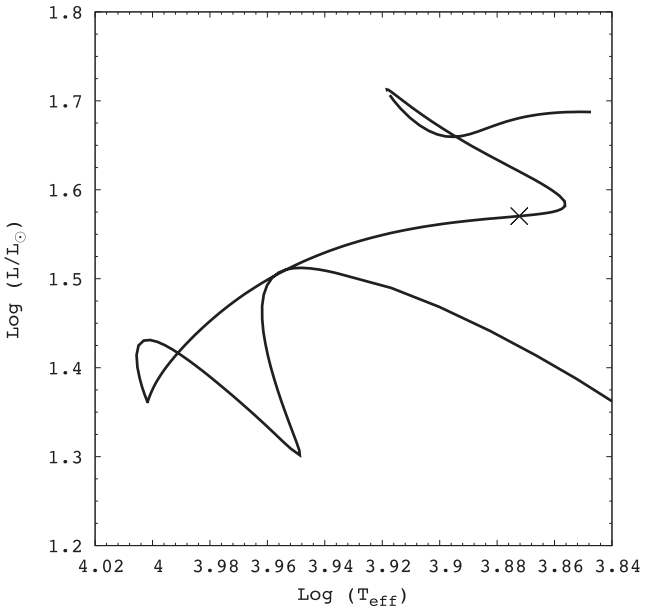

Figure 6. Position of the best model on its evolutionary track in the HR diagram, showing the evolutionary stage of the star. As this is a model, there are no error bars.

be unstable and (3) the global parameters should be inside the observational photometric error box. In Table 3 we show the main properties of the best obtained model. All the parameters are within the spectroscopic uncertainties. We show the star's position on the HR diagram and its evolutionary stage in Fig. 6.

Some important results come out from our comparison between theoretical time-dependent convection models and observations. First, we managed to obtain a model where seven of the eight highest amplitude frequencies are excited. The lowest frequency mode ($f_8 = 0.394\,48\,{\rm d}^{-1}$) is predicted to be stable (i.e. not excited). This mode might not be caused by oscillation – at these low frequencies, instrumental origins are common (Murphy 2012, his fig. 3). The origin does not appear to be rotational or equal to the difference in frequency between any two other modes in Table 4. The alternative to instrumental origin is that it is indeed a pulsation frequency, in which case the conclusion is that some physics is missing from the model. We did not model all 40+ statistically significant frequencies due to the overwhelming complexity involved in doing so.

Secondly, we found that the value of the mixing-length parameter giving the maximum value for the likelihood function is $\alpha_{\rm MLT} = 2$, i.e. different from the solar value in Grigahcène et al. (2012). It is known that $\alpha_{\rm MLT}$ should vary from star to star and also with temperature as the internal structure changes from a solar-like one to those of A- and F-stars. As this star is the first δ Sct star to be treated with TDC models, coverage of $\alpha_{\rm MLT}$ for $T_{\rm eff} > 6000$ K is currently unavailable, but for cooler stars we refer the reader to the works of Grigahcène et al. (2012) and Trampedach & Stein (2011) for deeper discussion.

Table 4. Identification of oscillating modes. Negative n values denote mixed modes with g-mode-like character. An additional observed frequency, $f_8 = 0.394\,48\,{\rm d}^{-1}$, was modelled but was not found to be excited. Formal least-squares frequency precision is $3 \times 10^{-6}\,{\rm d}^{-1}$ for f_1 and f_2, and $2 \times 10^{-5}\,{\rm d}^{-1}$ for f_3. Since our models do not include rotation to lift the degeneracy, all modes presented are $m = 0$.

ID	$f_{\rm Obs}$ ($\rm d^{-1}$)	ℓ	n	$f_{\rm Theo}$ ($\rm d^{-1}$)	$f_{\rm Obs} - f_{\rm Theo}$ ($\rm d^{-1}$)
1	10.337 59	0.0	3.0	10.364 43	−0.026 84
		1.0	0.0	10.451 43	−0.113 84
		3.0	−3.0	10.221 46	0.116 13
		2.0	−1.0	10.507 85	−0.170 27
2	12.471 61	0.0	4.0	12.471 6063	2.0E−07
		3.0	−1.0	12.455 54	0.016 07
3	10.936 41	3.0	−2.0	10.933 05	0.003 36
		1.0	1.0	10.943 67	−0.007 25
4	9.712 14	3.0	−4.0	9.711 85	0.000 29
		2.0	−2.0	9.719 28	−0.007 14
5	12.650 66	1.0	2.0	12.825 01	−0.174 35
		0.0	4.0	12.471 61	0.179 05
		3.0	−1.0	12.455 54	0.195 12
		2.0	1.0	12.892 38	−0.241 72
6	13.502 29	3.0	0.0	13.673 04	−0.170 74
7	11.482 87	2.0	0.0	11.657 46	−0.174 59

A third remark regards the fitting of the frequency values. In Table 4 we list the theoretical frequencies together with the observed frequencies and mode identifications. Four of the observed frequencies are very well fitted by the theoretical modes – the difference is less than $0.03\,{\rm d}^{-1}$ (0.35 μHz). For the other three the difference is less than $0.2\,{\rm d}^{-1}$. However, an ambiguity arises for some modes in that there are multiple mode identification possibilities of similar likelihood. This indicates that ground-based multicolour photometric or spectroscopic observation campaigns are necessary to complete the mode identification.

Finally, while the asteroseismic effective temperature agrees with the spectroscopic one to within less than 2σ, the $\log g$ value from the models (3.65) does not agree particularly well with that from spectroscopy (3.0 ± 0.1). Similar model behaviour was seen in Grigahcène et al. (2012).

6.2 Conclusions from modelling

We have compared the observed frequencies of KIC 3429637 to state-of-the-art δ Sct models. The results of this comparison are the following. (1) All the observed modes (those listed in Table 4) are predicted to be excited in our model except the lowest frequency. (2) Four out of seven frequencies are fitted to within 0.26 per cent. (3) The varying amplitudes between quarters might be explained by mode interaction – the modelled frequencies are all rather close and are perhaps subject to resonances as described in e.g. Dziembowski & Krolikowska (1985). We identify many potential mixed modes, and it is noteworthy that g modes that are not even visible in the

Fourier transform have the potential to affect p-mode frequencies (Buchler, Goupil & Hansen 1997).

7 CONCLUSIONS

The high-precision *Kepler* data indicate two dominant modes of growing amplitude, with different growth rates, and a third mode of intermediate amplitude whose amplitude decreases. The mode amplitude growth appears to be intrinsic to the star.

Our spectroscopic data confirm literature classifications that this star is of the marginal Am type. The heavy elements are overabundant with respect to solar values, and the light elements are underabundant – as one expects for Am stars. Notably, calcium is normal.

Mode amplitudes in δ Sct stars can change by large amounts on short time-scales, with changing growth rates (cf. 4 CVn). The amplitude growth in this star appears much less chaotic than for 4 CVn, and we have proposed evolution as the dominant cause, in that pulsation amplitudes are expected to increase naturally in evolving Am stars as the He II convection zone deepens and picks up residual helium. We cannot definitively rule out that mode interaction is the cause, where energy is being transferred from one or more modes into those whose amplitudes are growing, except to say that we see no modes decreasing in amplitude by comparable amounts to those by which the dominant modes are growing. As such, this explanation seems viable only if one or more unseen modes – perhaps g modes or high-degree p modes – are transferring the energy.

For the first time, time-dependent convection has been used in models of a δ Sct star observed with *Kepler*. Despite the narrow observational constraints, the modelling was difficult. We determine a 2.18 $M_{\odot}$, 7450-K model with $Z = 0.0149$ to be the best solution (cf. Table 3), with the star being 94 per cent of the way through its main-sequence lifetime (see Fig. 6), and we match four of seven mode frequencies to within 0.26 per cent (Table 4). Multicolour photometry and/or time series spectroscopy would facilitate mode identification, and this target is most worthy of continual follow-up in *Kepler*'s LC mode, not least because it offers a chance to witness stellar evolution on human time-scales.

ACKNOWLEDGMENTS

This research has made use of the SIMBAD data base, operated at CDS, Strasbourg, France. Calculations have been partially carried out in Wroclaw Centre for Networking and Supercomputing (http://www.wcss.wroc.pl), grant No. 214. Based on data from the *Kepler Space Telescope*, for which we are extremely grateful, and on observations made with the Nordic Optical Telescope, operated on the island of La Palma jointly by Denmark, Finland, Iceland, Norway and Sweden, in the Spanish Observatorio del Roque de los Muchachos of the Instituto de Astrofísica de Canarias (IAC).

SJM would like to acknowledge the financial support of the STFC. AG acknowledges the KITP staff of UCSB for their warm hospitality during the research programme 'Asteroseismology in the Space Age'. This research was supported in part by the National Science Foundation of the United States under Grant No. NSF PHY05-51164. EN acknowledges support from Polish MNiSW5 grant N N203 405139. KU acknowledges financial support by the Spanish National Plan of R&D for 2010, project AYA2010-17803. We thank the Spanish Night-Time Allocation Committee (CAT) for awarding time to the proposal 61-NOT7/10A.

REFERENCES

Abt H. A., 1979, ApJ, 230, 485
Abt H. A., 1984, ApJ, 285, 247
Abt H. A., 2009, AJ, 138, 28
Abt H. A., Morrell N. I., 1995, ApJS, 99, 135
Alexander D. R., Ferguson J. W., 1994, ApJ, 437, 879
Asplund M., Grevesse N., Sauval A. J., Scott P., 2009, ARA&A, 47, 481
Baglin A., Breger M., Chevalier C., Hauck B., Le Contel J. M., Sareyan J. P., Valtier J. C., 1973, A&A, 23, 221
Balona L. A. et al., 2011a, MNRAS, 413, 2403
Balona L. A. et al., 2011b, MNRAS, 414, 792
Boesgaard A. M., Friel E. D., 1990, ApJ, 351, 467
Böhm-Vitense E., 1958, Zeit. Astrophys., 46, 108
Breger M., 2000, in Szabados L., Kurtz D., eds, ASP Conf. Ser. Vol. 203, IAU Colloq. 176: The Impact of Large-Scale Surveys on Pulsating Star Research. Astron. Soc. Pac., San Francisco, p. 421
Brown T. M., Latham D. W., Everett M. E., Esquerdo G. A., 2011, AJ, 142, 112
Buchler J. R., Goupil M., Hansen C. J., 1997, A&A, 321, 159
Carrera R., Pancino E., 2011, A&A, 535, A30
Castelli F., Hubrig S., 2004, A&A, 425, 263
Catanzaro G., Balona L. A., 2012, MNRAS, 421, 1222
Catanzaro G. et al., 2011, MNRAS, 411, 1167
Chambers J. E., 2010, ApJ, 724, 92
Christensen-Dalsgaard J., Daeppen W., 1992, A&AR, 4, 267
Conti P. S., 1965, ApJ, 142, 1594
Conti P. S., 1970, PASP, 82, 781
Coupry M. F., Burkhart C., 1992, A&AS, 95, 41
Cox A. N., Hodson S. W., King D. S., 1979, ApJ, 231, 798
Crawford D. L., 1979, AJ, 84, 1858
Debernardi Y., 2000, in Reipurth B., Zinnecker H., eds, IAU Symp. 200, The Formation of Binary Stars. Astron. Soc. Pac., San Francisco, p. 161
Dommanget J., Nys O., 1994, Communications de l'Observatoire Royal de Belgique, 115, 1
Draper P. W., Allan A., Berry D. S., Currie M. J., Giaretta D., Rankin S., Gray N., Taylor M. B., 2005, in Shopbell P., Britton M., Ebert R., eds, ASP Conf. Ser. Vol. 347, Astronomical Data Analysis Software and Systems XIV. Astron. Soc. Pac., San Francisco, p. 22
Dupret M. A., 2001, A&A, 366, 166
Dupret M.-A., Grigahcène A., Garrido R., De Ridder J., Scuflaire R., Gabriel M., 2005, MNRAS, 361, 476
Dupret M.-A., Grigahcène A., Garrido R., Gabriel M., Scuflaire R., 2004, A&A, 414, L17
Dziembowski W., Krolikowska M., 1985, Acta Astron., 35, 5
Fossati L., Bagnulo S., Landstreet J., Wade G., Kochukhov O., Monier R., Weiss W., Gebran M., 2008a, A&A, 483, 891
Fossati L., Kolenberg K., Reegen P., Weiss W., 2008b, A&A, 485, 257
Gabriel M., 1996, Bull. Astron. Soc. India, 24, 233
Gebran M., Monier R., 2007, in Kupka F., Roxburgh I., Chan K., eds, IAU Symp. 239, Convection in Astrophysics. Cambridge Univ. Press, Cambridge, p. 160
Gebran M., Monier R., Richard O., 2008, A&A, 479, 189
Gebran M., Vick M., Monier R., Fossati L., 2010, A&A, 523, A71
Gilliland R. L. et al., 2010, PASP, 122, 131
Gray D. F., 2005, The Observation and Analysis of Stellar Photospheres. Cambridge Univ. Press, Cambridge
Gray R. O., Garrison R. F., 1989, ApJS, 69, 301
Grevesse N., Noels A., 1993, in Prantzos N., Vangioni-Flam E., Casse M., eds, Origin and Evolution of the Elements. Cambridge Univ. Press, Cambridge, p. 15
Grevesse N., Sauval A. J., 1998, Space Sci. Rev., 85, 161
Grigahcène A., Dupret M.-A., Sousa S. G., Monteiro M. J. P. F. G., Garrido R., Scuflaire R., Gabriel M., 2012, MNRAS, 422, L43
Hauck B., Mermilliod M., 1998, A&AS, 129, 431
Hill G. M., Landstreet J. D., 1993, A&A, 276, 142
Iglesias C. A., Rogers F. J., 1996, ApJ, 464, 943
Kallinger T., Matthews J. M., 2010, ApJ, 711, L35

Koch D. G. et al., 2010, ApJ, 713, L79
Kurtz D. W., 1976, ApJS, 32, 651
Kurtz D. W., 1978, ApJ, 221, 869
Kurtz D. W., 1989, MNRAS, 238, 1077
Kurtz D. W., 2000, in Breger M., Montgomery M., eds, ASP Conf. Ser. Vol. 210, Delta Scuti and Related Stars. Astron. Soc. Pac., San Francisco, p. 287
Kurtz D. W., Garrison R. F., Koen C., Hofmann G. F., Viranna N. B., 1995, MNRAS, 276, 199
Kurucz R., 1993a, Kurucz CD-ROM No. 13, ATLAS9 Stellar Atmosphere Programs and 2 km s^{-1} Grid. Smithsonian Astrophysical Observatory, Cambridge, MA
Kurucz R., 1993b, SYNTHE Spectrum Synthesis Programs and Line Data. Kurucz CD-ROM No. 18. Smithsonian Astrophysical Observatory, Cambridge, MA
Latham D. W., Brown T. M., Monet D. G., Everett M., Esquerdo G. A., Hergenrother C. W., 2005, BAAS, 37, 110.13
Lenz P., Breger M., 2004, in Zverko J., Ziznovsky J., Adelman S. J., Weiss W. W., eds, IAU Symp. 224, The A-Star Puzzle. Cambridge Univ. Press, Cambridge, p. 786
Mashonkina L., Korn A. J., Przybilla N., 2007, A&A, 461, 261
Meléndez J., Asplund M., Gustafsson B., Yong D., 2009, ApJ, 704, L66
Michaud G., Richer J., Richard O., 2005, ApJ, 623, 442
Murphy S. J., 2012, MNRAS, 422, 665
Niemczura E., Morel T., Aerts C., 2009, A&A, 506, 213
Olsen E. H., 1983, A&AS, 54, 55
Pace G., Recio-Blanco A., Piotto G., Momany Y., 2006, A&A, 452, 493
Ramírez I., Meléndez J., Asplund M., 2009, A&A, 508, L17
Rentzsch-Holm I., 1996, A&A, 312, 966
Sbordone L., 2005, Mem. Soc. Astron. Ital. Suppl., 8, 61
Scuflaire R., Théado S., Montalbán J., Miglio A., Bourge P.-O., Godart M., Thoul A., Noels A., 2008, Ap&SS, 316, 83
Shibahashi H., Kurtz D. W., 2012, MNRAS, 422, 738
Smalley B. et al., 2011, A&A, 535, A3
Smith J. C. et al., 2012, PASP, 124, 1000
Smith M. A., 1970, ApJ, 161, 1181
Smith M. A., 1973, ApJS, 25, 277
Stateva I., Iliev I. K., Budaj J., 2012, MNRAS, 420, 1207
Stumpe M. C. et al., 2012, PASP, 124, 985
Takeda Y., Han I., Kang D. I., Lee B.-C., Kim K.-M., 2008, J. Korean Astron. Soc., 41, 83
Templeton M., Basu S., Demarque P., 2002, ApJ, 576, 963
Trampedach R., Stein R. F., 2011, ApJ, 731, 78
Turcotte S., Richer J., Michaud G., Christensen-Dalsgaard J., 2000, A&A, 360, 603
Uytterhoeven K. et al., 2011, A&A, 534, A125
van't Veer-Menneret C., Megessier C., 1996, A&A, 309, 879
Varenne O., Monier R., 1999, A&A, 351, 247
Zahn J.-P., 1975, A&A, 41, 329

This paper has been typeset from a TEX/LATEX file prepared by the author.